Enzyme-Catalyzed Gel Proteolysis: An Anomalous Diffusion-Controlled Mechanism

G. C. Fadda,* D. Lairez,* B. Arrio,† J.-P. Carton,‡ and V. Larreta-Garde§

*Laboratoire Léon Brillouin, Commissariat à l'Energie Atomique/Saclay, Gif-sur-Yvette, France; †Laboratoire de Photophysique Moléculaire, Université Paris-Sud, Orsay, France; ‡Laboratoire de Physique de l'État Condensé, Commissariat à l'Energie Atomique/Saclay, Gif-sur-Yvette, France; and §Équipe de Recherche Relations Matrice Extracellulaire, Université de Cergy-Pontoise, Cergy-Pontoise, France

ABSTRACT Enzyme-catalyzed proteolysis of gelatin gels has been studied. We report a gel degradation rate varying as the square of the enzyme concentration. The diffusion motion of enzymes in the gel has been measured by two-photon fluorescence correlation spectroscopy and identified as being anomalously slow. These experimental results are discussed from a theoretical point of view and interpreted in terms of a diffusion-controlled mechanism for the gel degradation. These results make a step toward the understanding of enzyme-catalyzed gel degradation and give new insight on biological processes such as the action of metalloproteinases in the extracellular matrix involved in cellular invasion.

INTRODUCTION

In vivo, proteins are often organized in a gel state, i.e., an elastic solid of macromolecules swollen by a large amount of solvent. On one side, protein gelation is involved in many biological processes such as blood coagulation or wound healing (Furie and Furie, 1988). Conversely, the transition from a gel and solid state to a soluble and liquid state is also of major importance, mainly for the extracellular matrix (ECM) behavior. The ECM is a gel of various functional and structural macromolecules (mainly collagen, a high molecular weight protein) with acute roles in physiology. ECM constitutes a physical barrier isolating organs and is an essential regulator of cell behaviors (Basbaum and Werb, 1996; Assoian, 1997). In tumor dissemination, invasive cells must solubilize the ECM gel (Bissell and Radisky, 2001). This degradation involves up to 15 different proteolytic enzymes, especially metalloproteinases (MMP), the expression of which have been correlated with tumor invasiveness (Murphy and Gavrilovic, 1999; DeClerck, 2000; McCawley and Matrisian, 2000). These proteinases differ by their specificities and reaction mechanisms; moreover, the ECM composition and organization are tissue-dependent. Despite these peculiarities, in all cases cell invasion implies a similar process that requires the enzyme-catalyzed degradation of the ECM gel. Beyond the precise biochemical processes involved at a molecular level, the understanding of the physical mechanisms of the degradation is crucial. From this point of view, the use of simplified model systems is an unavoidable stage within the present state of the art.

The ECM degradation in relation with cell invasion has been widely modeled and considered from a theoretical point of view (Dallon et al., 1999; Perumpanani and Byrne, 1999), but very few studies have actually been devoted to enzyme kinetics in the corresponding heterogeneous and insoluble media (Berry and Larreta-Garde, 1999; Larreta-Garde and Berry, 2002). Experimentally, kinetics of enzyme-catalyzed degradation of ECM gels has been reported only recently (Berry et al., 2000), but the corresponding physical mechanism of degradation still remained puzzling.

In this article, we report an experimental study which makes a step toward the understanding of this mechanism. Thermolysin-catalyzed degradation of gelatin gels has been considered as a model system. Gelatin is denatured collagen, the main ECM constituent. The gel network crosslinking is due to partial renaturation and triple helix formation (Djabourov et al., 1993). Thermolysin is a Zn-metalloproteinase from Bacillus thermoproteolyticus which is an analog of MMP and displays the same basic mechanism (Browner et al., 1995; Grams et al., 1995), but without the need of other enzymes for activation and with a better stability. Enzyme concentrations in this study are in the range of 1 nM, which is the order of magnitude of MMP concentration in ECM during cell invasion (Berry and Larreta-Garde, 1999).

The experimental study here reported consists of two parts: 1), the enzyme-concentration dependence of the gel degradation rate; and 2), the two-photon fluorescence correlation spectroscopy study of the thermally induced motion of the enzyme in the gel. In the last part of the article, these results are discussed from a theoretical point of view. We will see how these data suggest a degradation mechanism controlled by an anomalous diffusion of the enzyme in the gel.

MATERIALS AND METHODS

Sample preparation

Gelatin of type B from bovine skin was purchased from Sigma (G9382, Billerica, MA). Gelatin solution was prepared in 50 mM Tris-HCl buffer at pH = 7.4 at 40°C and filtered by 0.45 μm Millipore filters (Sigma-Aldrich, St. Louis, MO). Gel point determinations were performed by quasi-elastic light scattering (QELS) on diluted large latex probe particles (450-nm diameter; Fadda et al., 2001). For these experiments, polystyrene latex particles at a final volume fraction $\phi = 1.8\ 10^{-6}$ were added to the gelatin solution at a final concentration of 1% w/w. Thermolysin (Protease X Bacillus Rokko, EC 3-4-24-27) was purchased from Sigma (Lot No. 16H0855). Aliquots of 0.12 mg/ml

Submitted August 20, 2002, and accepted for publication June 10, 2003.

Address reprint requests to D. Lairez, Tel.: 33-16-908-7231; Fax: 33-16-908-8261; E-mail: lairez@cea.fr.

0006-3495/03/11/2808/10 $2.00

stock solution in pH = 7.4, 50 mM Tris·HCl buffer were used for QELS experiments and kept at $T = -20$°C. Thermolysin solution was added to the gelatin solution at 40°C (gelatin in a liquid state), stirred and cooled at 4°C for 1 h to accelerate the gelation process. The gel was then warmed at 14°C in the experimental device for measurements.

Thermolysin labeling

Fluorescein isothiocyanate (FITC, isomer I) was purchased from Sigma. FITC reacts with primary amines of proteins to form a dye protein conjugate. FITC-thermolysin conjugate was prepared according to Molecular Probes (Eugene, OR) protocol. The excess of FITC was removed from protein solution by gel filtration on prepacked Sephadex G-25 column from Pharmacia (Pharmacia-Pfizer, Mississauga, Canada). Final thermolysin concentration was calculated from absorbance measurements at 280 nm (A_{280}) and 494 nm (A_{494}) of the purified conjugate: $[thermolysin](M) = [A_{280} - (A_{494} \times 0.30)]/\varepsilon$, where $\varepsilon = 6.61 \times 10^4\ cm^{-1}\ M^{-1}$ is the molar extinction coefficient of thermolysin at 280 nm and 0.30 is a correction factor accounting for the absorption of FITC at 280 nm. The degree of labeling L (number of FITC per protein molecule) was calculated as $L = A_{494}/(6.8 \times 10^4 \times [thermolysin])$, where $6.8 \times 10^4\ cm^{-1}\ M^{-1}$ is the molar extinction coefficient of FITC at 494 nm and pH = 8. In our experiment $L = 2.7$.

Thermolysin stability

100 nM thermolysin were stored at 10°C in gelatin solutions at 0.5% and 0.1%. Samples of these preparations were tested for proteolytic activity on a peptidic substrate, FA-Gly-Leu (final concentration 1.6 mM), in a Tris 50 mM Maleate buffer pH = 7.0 containing 10 mM $CaCl_2$. The reaction was followed by optical density measurements at 345 nm ($\varepsilon_{345} = 660\ M^{-1}\ cm^{-1}$).

Two-photon fluorescence correlation spectroscopy

Routinely (Guiot et al., 2000), two-photon fluorescence excitation mode was performed with a Coherent (Santa Clara, CA) Titanium sapphire model 900 Mira laser head, modelocked and tunable from 710 to 920 nm. The Mira laser head was pumped by a 5-W solid-state Coherent laser model Verdi providing a single frequency output of 532 nm. The excitation beam tuned at 824 nm had an integrated power of 3 mW. It replaced the light source of an Axiovert 135 inverted microscope from Zeiss (Oberkochen, Germany), equipped with an immersion objective 63×, NA 1.4. A dichroic beam splitter separated the epifluorescent and excitation beams. Fluorescence was detected at 520 nm by a Hamamatsu model R7205-01 photomultiplier (Sunayama, Japan). The fluorescence intensity autocorrelation function was calculated by a multi-tau digital correlator Flex2K-12 × 2 from Correlator.com (Bridgewater, NJ). For each spectra, the baseline is computed with an accuracy of 10^{-4} from the squared mean fluorescence intensity averaged over the experiment duration. At long time, all correlation functions here reported reach the baseline within 10^{-3} accuracy. Nonlinear fitting of data (without data point weighting) was performed using the Levenberg-Marquardt algorithm to search for the minimum value of χ^2. Errors bars reported for the so-determined fitting parameters correspond to the standard deviations calculated using the residual to estimate the error bar for each data point.

Compared to standard confocal experimental setup for fluorescence correlation spectroscopy, the two-photon technique has the major advantage to limit photobleaching to the detection volume around the waist of the laser beam.

RESULTS

Gel degradation kinetics

Here we report data on the degradation of a protein gel under the action of proteinase. The gel is an aqueous solution of gelatin at a weight fraction of 1% that becomes solid (gel) at low temperature (see Method). Under the action of proteinase some peptide bonds belonging to gelatin chain connecting two crosslinks of the gel network are hydrolyzed and the gel becomes liquid as a given fraction of such bonds are broken. In that sense, the gel undergoes a reverse sol-gel transition (Adam and Lairez, 1996); however, in this article, we are not concerned with the study of the critical behavior of the transition, but only with the reverse-gel time t_{gel}.

This time was determined using an experimental method already reported (Fadda et al., 2001). It consists in QELS measurements on diluted large latex probe particles (450 nm diameter): in the gel state, due to the shear elastic modulus, fluctuations of light-scattered intensity are frozen and the amplitude of these fluctuations increases as the shear elastic modulus vanishes due to the action of proteinase. At the gel point in the liquid state, t_{gel}, one recovers the amplitude of fluctuation measured in water. Results so obtained are reported in Fig. 1 for different enzyme concentrations between 0.6 nM and 4 nM. The gel degradation time is found to vary with the enzyme concentration as

$$t_{gel} = 120 \times [E]^{1.95 \pm 0.15}, \quad (1)$$

where t_{gel} is expressed in hours and $[E]$ in nM.

The gel degradation kinetics is very slow at these proteinase concentrations: the gel time reaches 10 days at the lowest concentration. In view of these long times, the QELS method used for the determination of t_{gel} shows a number of advantages compared to usual rheological measurements: samples are in sealed measurement cells, allowing temperature regulation and preventing contamination and solvent evaporation. As measurements are

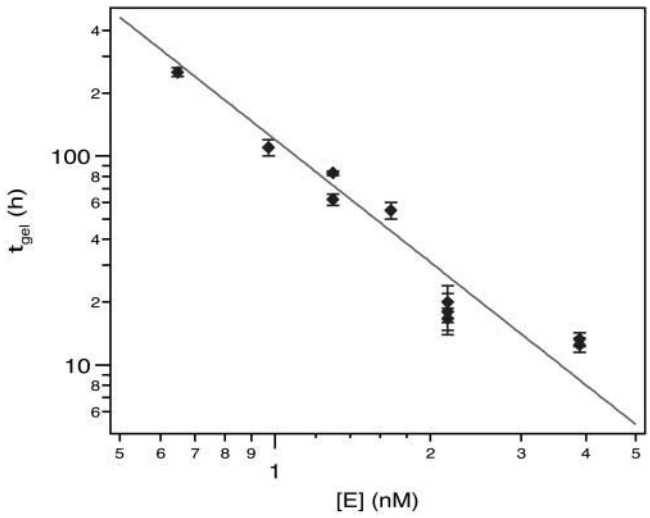

FIGURE 1 Variation of the gel proteolysis time, t_{gel}, on enzyme concentration, $[E]$. The straight line has a slope in *log-log* = −1.95 ± 0.15.

performed for very long time, the stability of the enzyme is questionable. Thermolysin is known to be a particularly stable enzyme (Imanaka et al., 1986). However, to check this point, especially in the presence of gelatin, i.e., a substrate for the enzyme, thermolysin activity was measured at different times on two solutions at different gelatin concentrations. Results are reported in Table 1. It appears that the presence of gelatin reinforces the enzyme stability: at gelatin concentration of 0.5% the enzyme activity is constant within experimental accuracy. In addition, this result shows that at these low enzyme concentrations a decreasing proteinase activity of thermolysin due to autolysis is negligible. As a consequence, results plotted in Fig. 1 have to be compared to theoretical expectation for the enzyme-catalyzed gel degradation mechanism.

We will see in the following (see Discussion) that a classical Michaelis-Menten formalism leads us to expect a gel degradation rate proportional to $[E]$. To explain the $[E]^2$ dependence here reported, a degradation mechanism controlled by an anomalous slow diffusion of the enzyme in the gel may be considered.

Enzyme-diffusion measurements by two-photon fluorescence correlation spectroscopy

To get direct evidence of slow diffusion of enzymes in the gel, fluorescence correlation spectroscopy (FCS) measurements were performed. To our knowledge, this is the only technique for such measurements. On the one hand, enzymes are too small to allow QELS measurements, especially because the gel has a major contribution to the scattered light intensity; working on labeled enzymes is a major advantage of fluorescence techniques. On the other hand, the technique of fluorescence recovery after photobleaching works in a higher concentration range of fluorescent molecules.

FCS consists of computing the correlation function of the fluorescence intensity, I, of a small volume observed with a confocal or two-photon microscope (Krichevsky and Bonnet, 2002). In the absence of chemical fluctuations, FCS is directly sensitive to concentration fluctuations of fluorescent markers due to their translational motion. In practice, the measured signal is a convolution of correlation function of concentration fluctuations with the excitation volume profile, leading to complex relaxation function. For reasons of straightforwardness of the calculation, a Gaussian excitation profile is often assumed (Krichevsky and Bonnet, 2002). In this case, a two-dimensional profile in the x-y plane leads to the correlation function of the fluorescence intensity,

$$G(t) = \frac{\langle I(0)I(\tau)\rangle}{\langle I\rangle^2} - 1 = \frac{\langle \Delta I(0)\Delta I(\tau)\rangle}{\langle I\rangle^2} = \frac{1}{N}\left(1 + \frac{t}{\tau}\right)^{-1}, \tag{2}$$

where N is the number of excited molecules in the observed area, $\tau = {L_{xy}}^2/4D$ is the diffusion characteristic time of such labeled molecules across the ${L_{xy}}^2$ excitation area, and D their diffusion coefficient. However, diffusion can also occur along the z-axis leading to the more complex expression,

$$G(t) = \frac{1}{N}\left(1 + \frac{t}{\tau}\right)^{-1}\left(1 + \frac{t}{\omega^2\tau}\right)^{-1/2}, \tag{3}$$

where $\omega^2 = {L_z}^2/{L_{xy}}^2$ is the aspect ratio of the excitation volume that is assumed to have a Gaussian profile along the three axis (Krichevsky and Bonnet, 2002). In practice, this is not necessarily the case for a given experimental setup and phenomenological expressions can better account for the data. To estimate such an apparatus function, measurements in simple liquid were first performed.

Measurements on fluorescent latex particles and labeled enzymes in simple liquids

Fluorescent latex particles were characterized by quasi-elastic light scattering measurements. The so measured dynamical structure factor of these particles is accounted for using a simple exponential decay. The corresponding diffusion coefficient, D_{latex}, is found to be independent of the scattering angle between 40° and 140°, and is equal to $D_{\text{latex}} = (7.7 \pm 0.8) \times 10^{-8}$ cm^2/s. From the Stokes-Einstein relation $D = kT/6\pi\eta R_{\text{H}}$, where kT is the thermal energy, η the solvent viscosity, and R_{H} the hydrodynamic radius, one gets $R_{\text{H latex}} = (28.2 \pm 0.3)$ nm.

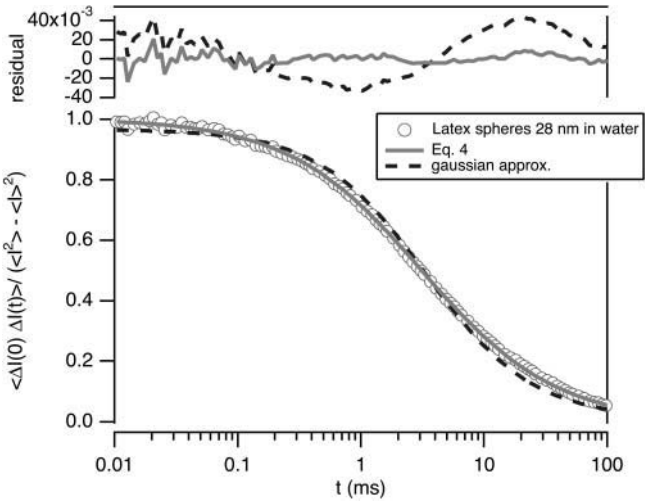

FIGURE 2 Normalized fluorescence correlation function versus time for 28-nm radius latex beads in water. The lines correspond to the best fits using Eq. 3 (*dashed line*), which assumes a Gaussian observation volume and the phenomenological Eq. 4 (*solid line*), respectively. Fit residuals are plotted on the top of the graph.

TABLE 1 Thermolysin proteolysis activity (μM × min^{-1})

t (h)	0	41	118
Gelatin 0.1%, $[E] = 100$ nM	10.4	10.4	5.7
Gelatin 0.5%, $[E] = 100$ nM	4.8	5.0	5.1

In Fig. 2, the normalized correlation function of fluorescence intensity is plotted for these labeled latex particles in dilute solution in pure water. Normalization is performed dividing the correlation function, $G(t)$, by the amplitude of the fluctuations $A = \langle I^2\rangle/\langle I\rangle^2 - 1$, which is typically of the order of 3×10^{-2} for these measurements on latex particles in water. For this sample one expects a relaxation curve due to a simple diffusion process only. In Fig. 2, data are fitted using the corresponding relaxation function assuming a Gaussian profile for the excitation volume (Eq. 3). A systematic deviation of the fit is observed (see residual on top of the figure). Such distortion compared to the ideal case has been widely addressed in a recent article (Hess and Hebb, 2002). In the case of one-photon fluorescence spectrometers that use a pinhole to limit the extend of the observation volume, diffraction fringes due to the objective back aperture are mainly responsible for this distortion. With two-photon fluorescence, the observation volume is intrinsically limited without the need of pinhole. However, even in this case, the observation volume can be distorted from imperfect beam collimation and aberrations of the lens. The amplitude of the fit residual plotted in Fig. 2 is of the same order of magnitude as the one already reported for two-photon FCS (Hess and Hebb, 2002).

To avoid a bad interpretation of the data, that should be based on the wrong assumption that the observation volume is Gaussian, we tried to used a phenomenological expression for the relaxation function that would account for simple diffusion. In the whole time range the correlation function is nicely fitted using a two-parameters' expression of the form

$$g(t) = \frac{\langle \Delta I(0) \times \Delta I(\tau)\rangle}{\langle I^2\rangle - \langle I\rangle^2} = \left(1 + \left(\frac{t}{\tau}\right)^{\alpha}\right)^{-1}. \qquad (4)$$

The best fit leads to $\alpha = 0.81 \pm 0.02$ and $\tau = (3.10 \pm 0.05)$ ms, for latex spheres of 28-nm radius in water. The α-value indicates a broader profile of the observation window than in the ideal case; at long time, the relaxation function decreases more slowly than $t^{-3/2}$, as expected from Eq. 3. Note that this long-time behavior rules out a possible distortion of the relaxation function from photobleaching, which would result in an exponential cutoff in the relaxation function and thus to a function decreasing more quickly than $t^{-3/2}$. In the following paragraph, viscosity effect reported on enzyme measurements will give further evidence that Eq. 4 with a fixed value of $\alpha = 0.81$ acts as an apparatus function accounting for simple diffusion. The characteristic time τ found for latex particles in water allows us to calculate the length, $L = \sqrt{6D_{\text{latex}}\tau} = (380 \pm 20)$ nm, characteristic of the apparatus, which gives an estimation of the size of the fluorescence excitation volume.

FCS measurements were performed for 33.5 nM labeled thermolysin in water and in 50% glycerol solution. The shape of the spectra is accounted for using Eq. 4 with the imposed value of $\alpha = 0.81$ determined on latex particles data. The amplitude of the fluctuations is determined by fitting the spectra with Eq. 4 using an amplitude as an additional free parameter. In both cases, the amplitude is the same within error bars and equals $(2.8 \pm 0.4) \times 10^{-2}$. Spectra can thus be normalized in the same manner as in Fig. 2. Results are plotted in Fig. 3 in *log-lin* and *log-log* scale to emphasize the long time part of the spectra. Knowing that the solvent viscosity, η, is 12× higher than in water, measurements in 50% glycerol superimpose to those in water. Measurements in water and glycerol solution are thus consistent with a simple diffusion motion governed by Stokes-Einstein equation. This can be checked considering the hydrodynamic radius of thermolysin that can be calculated from the $M^{1/3}$ dependence reported in literature for globular proteins: $R_H/M^{1/3} = 0.80 \pm 0.07$, with R_H expressed in nm and the molecular weight M in kg/mol (Creighton, 1997). The molecular weight of thermolysin ($M = 34.6$ kg/mol) leads to $R_{H,\text{thermolysin}} = (2.6 \pm 0.2)$ nm. With the hydrodynamic radius of latex particles being measured by quasi-elastic light scattering, the FCS spectra can be plotted using the reduced variable, $t_r = t(\eta_{\text{water}}R_{H,\text{Thermolysin}})/(\eta R_H)$, to account for the different viscosities and hydrodynamic radii. In Fig. 3, one can see that the spectra measured for thermolysin and latex spheres nicely superimpose on a single master curve written as

$$g(t) = 1/[1 + (t_r/[0.28 \pm 0.01])^{0.81}].$$

Fitting only the data obtained on thermolysin in water, one gets a slightly smaller correlation time of $\tau = (0.22 \pm 0.01)$ ms (instead of 0.28), which can be ascribed to a small

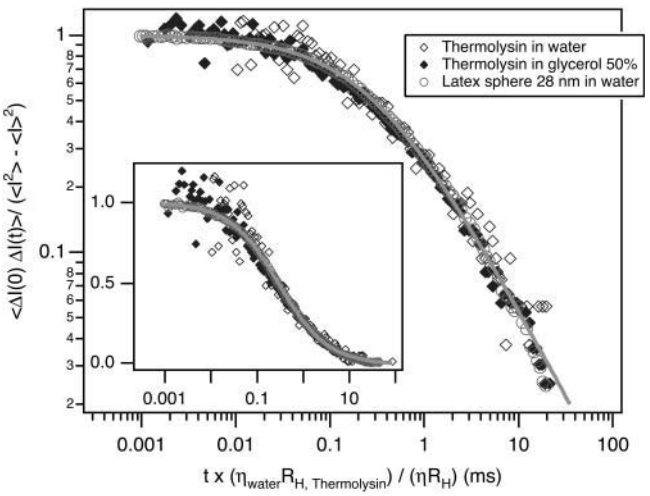

FIGURE 3 Normalized fluorescence correlation function measured for 28-nm radius latex beads in water (*circles*), for thermolysin in water (*open diamond*), and thermolysin in 50% glycerol solution (*full diamonds*), respectively. The abscises' axis uses the reduced variable, $t_r = t(\eta_{\text{water}}R_{H,\text{Thermolysin}})/(\eta R_H)$, to account for different solvent viscosities (η), and to diffuse hydrodynamic radii (R_H), and to rescale measurements to those obtained for thermolysin in water (see text). The line is the best fit using Eq. 4, with $\alpha = 0.81$.

amount of free fluorescent markers (FITC) still present in the labeled thermolysin solution. On the contrary, note that a partial thermolysin denaturation or aggregation leading to a polydispersity in the protein size would result to an increase of the corresponding time.

In summary, FCS measurements on fluorescent latex particles and labeled enzymes in simple liquids rescale correctly, once one has accounted for the liquid viscosity and the size of the fluorophore carrier. This clearly indicates that the measured fluorescence fluctuations are governed by diffusion processes and that the nonideal correlation curve is due to the apparatus function.

Measurements on fluorescent latex particles and labeled enzymes in gelatin gel

FCS measurements performed on latex particles in gelatin gel lead to the same relaxation profile as in water (see Fig. 4). Data are accounted for using Eq. 4 with the same value of α but with a longer relaxation time. In particular, the amplitude of fluctuation is of the same order of magnitude in both cases. This result shows that 28-nm beads are free to move in the gel and only experience a viscosity higher than in water. Actually, for this gel the correlation length of gelatin concentration fluctuations has been measured by light scattering equal to $\xi_T = (43 \pm 4)$ nm (Fadda et al., 2001). This is the lowest value expected for the mesh size, ξ_c, of a fully connected gelatin network at this concentration. Moreover, at this concentration and temperature, gelatin gels prepared in the same way display a shear elastic modulus, G, equal to 4.0 Pa (Gau, 2002). Assuming that the volume ξ_c^3 stores an elastic energy equal to kT, i.e., $G = kT/\xi_c^3$, one gets $\xi_c = 100$ nm. Thus, this estimate and FCS measurements on these latex particles are consistent with a gelatin network which does not trap the particles. As these latex particles are free to move in the gel, in the absence of specific interactions one expects, a fortiori, the same for thermolysin molecules, which are 10× smaller.

FCS measurements were performed for 6.7 nM labeled thermolysin in gelatin gel. Results are plotted in Fig. 5. In this figure, the line corresponds to the master curve obtained in Fig. 3 that accounts for the diffusion of thermolysin in water. Measurement obtained on thermolysin in gelatin gel (*triangles* in Fig. 5) cannot be easily extrapolated to $t = 0$. Thus, to avoid spectrum normalization, the master curve was rescaled by the ratio $A_{\text{simple liquid}} \times \langle I \rangle_{\text{simple liquid}} / \langle I \rangle_{\text{gel}}$, where $A_{\text{simple liquid}}$ is the amplitude of the correlation function measured for thermolysin in a simple liquid (water and/or glycerol solution), and $\langle I \rangle_{\text{simple liquid}}$ and $\langle I \rangle_{\text{gel}}$ would be the average fluorescence intensity measured in both cases. This aims to account for the $1/N$ dependence of the correlation function (Eqs. 2–3).

As opposed to the results obtained in simple liquids, measurements performed on labeled thermolysin in gelatin solution display a quite different shape for the relaxation function which decreases as a power law over five orders-of-magnitude in time. Translational motion of enzymes in the gel is clearly slowed down and anomalous compared to the behavior in water. An interpretation in terms of a distribution of the enzyme population can be ruled out. First, because such a distribution is not observed in a simple liquid (water

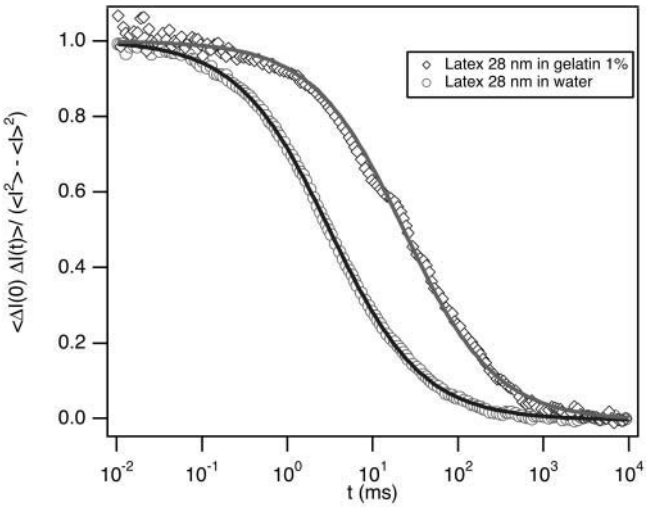

FIGURE 4 Normalized fluorescence correlation function versus time for 28-nm radius latex beads in water (*circles*) and gel (*diamonds*). The lines correspond to the best fits using Eq. 4 with $\alpha = 0.81 \pm 0.02$. For measurement in water, $\tau = (3.10 \pm 0.05)$ ms, whereas $\tau = (23.0 \pm 0.5)$ ms in gelatin. In both cases, latex particles experience a simple liquid viscosity and move through simple diffusion.

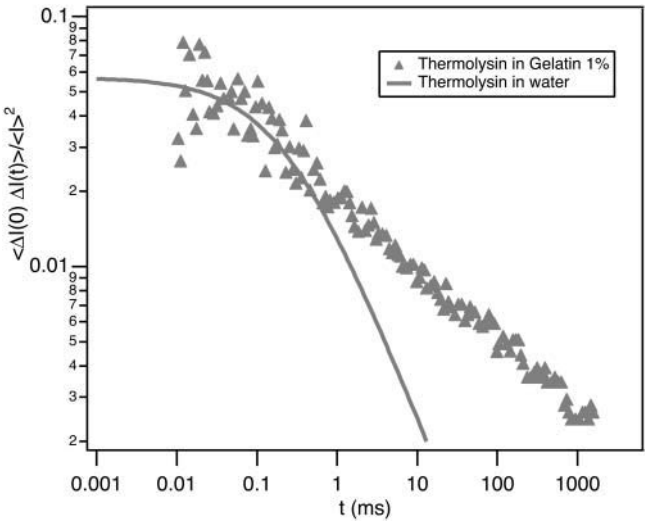

FIGURE 5 Fluorescence correlation function for thermolysin in gelatin gel (*triangles*) at the beginning of the degradation process. The line corresponds to the master curve obtained in Fig. 3 that accounts for the diffusion of thermolysin in water. The master curve was rescaled by the factor $A_{\text{simple liquid}} \times \langle I \rangle_{\text{simple liquid}} / \langle I \rangle_{\text{gel}}$, where $A_{\text{simple liquid}}$ is the amplitude of the correlation function measured for thermolysin in a simple liquid (water and/or glycerol solution), and $\langle I \rangle_{\text{simple liquid}}$ and $\langle I \rangle_{\text{gel}}$ the average fluorescence intensity measured in both cases.

or glycerol solution); and second, because fitting the FCS relaxation curve using a mode distribution leads to strong correlations in the residual (except with an arbitrary and unphysically high number of modes). To further advance the data interpretation, let us assume that the correlation function is only a function of the reduced mean square displacement, $\langle (r/L)^2 \rangle$, of enzyme, with L the length characteristic of the apparatus. This assumption implicitly assumes that there is only one population of labeled enzymes. Eq. 4 can be rewritten as $g(t) = [1+\langle (r/L) \rangle^{\alpha}]^{-1}$. Taking advantage of the simple form for $g(t)$, one easily gets

$$\left\langle \left[\frac{r}{L}\right]^2 \right\rangle = \left(\frac{1}{g(t)} - 1\right)^{1/\alpha}, \tag{5}$$

which leads to the time-dependent mean square displacement from measurements. Note that data interpretation, based on the mean square displacement so calculated, allows us to get rid of the particular shape of the apparatus function. Results are plotted in Fig. 6, where the straight line corresponds to the master curve plotted in Figs. 3 and 5, accounting for thermolysin diffusion in water. Compared to the diffusion in water, the diffusion in the gel is slowed down and the mean square displacement shows an anomalous time dependence: over three decades in time, one observes

$$\langle (r/L)^2 \rangle = (3.2 \pm 0.1) \times t^{0.40 \pm 0.01} \tag{6}$$

(see the *dashed line* in Fig. 6).

DISCUSSION

Classical Michaelis-Menten expectations

The enzyme kinetics of the gel degradation can first be considered in the framework of the classical Michaelis-Menten formalism that considers the mechanism

$$E + S \underset{k_{-1}}{\overset{k_{+1}}{\rightleftharpoons}} ES \overset{k_{\text{cat}}}{\rightarrow} E + P, \tag{7}$$

with S the enzyme substrate, i.e., a peptide bond of the gel, P a hydrolyzed peptide bond, and k_i the kinetic constant. In the stationary stage of the reaction, the concentration of Michaelis complexes is

$$[ES] = [E]_T/(1 + K_m/[S]), \tag{8}$$

where $[E]_T$ is the total enzyme concentration and $K_m = (k_{-1} + k_{\text{cat}})/k_{+1}$ is the Michaelis constant. The velocity, V, of the enzyme-catalyzed reaction is $V = d[P]/dt = k_{\text{cat}}[ES] = V_{\max}/(1 + K_m/[S])$, where $V_{\max}$ is the maximum velocity for saturated enzymes proportional to the enzyme concentration $V_{\max} = k_{\text{cat}}[E]$.

Gelatin is characterized by the repetition of Gly-X-Y sequences (Creighton, 1997) (where X and Y are variable amino acids). Considering the specificity of thermolysin (Matsubara, 1966) and the average composition of skin gelatins (Eastoe and Leach, 1977), 20% of total peptidic bonds can be recognized by the enzyme. For gelatin molecular mass of 10^5 g/mol corresponding to 1000 peptide bonds in average, the number of such recognition sites potentially breakable is thus of the order of 200 per gelatin chain. The gel is a network of crosslinks connected by gelatin chains. It has previously been shown (Fadda et al., 2001) that at the concentration here studied, gelatin chains are at the overlap concentration. This means there is, on the average, one chain per crosslink for a fully connected gel. Actually, this number is always less than unity and is found to be always <0.5 at the gelation threshold, both for percolation simulations (Clerc et al., 1983) and mean-field approach (Flory, 1953). From the point of view of the reverse sol-gel transition efficiency, the hydrolysis of one peptide bond of this crosslinking chain is enough; however, a lot of reaction sites remain on this broken chain as a substrate for the enzyme. Consequently, at the transition threshold between the gel and the liquid state, the substrate consumption never exceeds 1/200 of the initial value $[S]_0$. The substrate consumption is thus negligible up to the gel point. The consequence is that the velocity, V, of the enzyme-catalyzed reaction can be considered as constant up to the time t_{gel}. In other words t_{gel} is proportional to $1/V$. Now the importance of the result reported in Fig. 1 clearly appears. An ordinary Michaelis-Menten mechanism for the enzyme reaction would lead to $V \propto [E]$, whereas here $V \propto [E]^2$ is observed instead.

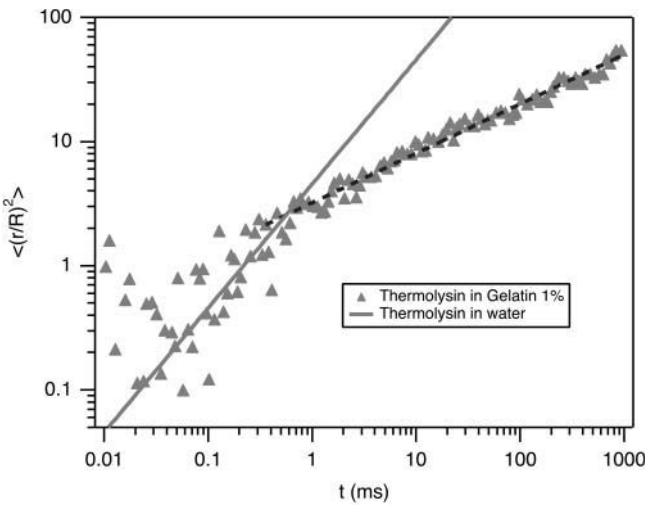

FIGURE 6 Reduced mean square displacement of thermolysin in the gel deduced from Eq. 5 and data reported in Fig. 5. Solid line corresponds to the master curve plotted in Figs. 3 and 5 that accounts for the diffusion of thermolysin in water. The dotted line corresponds to the power law of $\langle (r/L)^2 \rangle = (3.2 \pm 0.1) \times t^{0.40 \pm 0.01}$.

Enzyme diffusion and gel proteolysis

In regard to the physical properties, the gel proteolysis can be viewed as a reverse gelation process (Berry et al., 2000). In standard gelation models (Adam and Lairez, 1996), crosslinks are expected to occur (or to break in our case of

a reverse gelation) randomly with an equal probability anywhere in sample volume. In other words, it is assumed that there is no correlation between one crosslink formation (or breaking) and another. In our case, the breaking of crosslinks in the gel is due to the action of an enzyme and thus necessarily involves the enzyme diffusion in the gel. In that case, correlations cannot be ignored in the description of the gel degradation process because one given enzyme creates a liquid pathway in the gel.

For reason of simplicity, let us consider at $t = 0$ a fully connected network of mesh size $\xi_c = \xi_T$. Due to the action of enzyme, the correlation length, ξ_c, of the network connectivity will increase with time, but the length ξ_T can be considered as constant ($[S] \propto 1/{\xi_T}^3$). The time τ, needed for one gel network bond to be broken, is proportional to the time needed for the enzyme to move from one network mesh to an other, $\tau = {\xi_T}^2/D$, with D the effective diffusion coefficient of the enzyme. The probability, p, for one bond of the gel network to be unbroken, is time-dependent. The instantaneous rate of bonds breaking is $-dp/dt = {\xi_T}^3[E](1 - p)/\tau$, leading to

$$p(t) = exp(-\xi_T[E]Dt). \tag{9}$$

For a more rigorous expression and derivation, see Appendix. To evaluate the role of correlations in the gel degradation process, one can calculate the pair correlation function of the fluctuations of the unbroken bonds concentration, $C(r_{ij}, t) = \langle \delta x_i \delta x_j \rangle$, where x_i and x_j denote the unbroken bonds concentration in two points r_{ij} apart. One can show (see Appendix) that

$$C(r_{ij}, t) = \frac{C_0}{r_{ij}} \quad \text{with} \quad C_0 = p(t)^2 \xi_T[E]Dt. \tag{10}$$

The $1/r_{ij}$ behavior is reminiscent of that of the Debye function in polymer physics. This correlation function does not involve any characteristic length and slowly decreases with r_{ij}. Consequently we deal with a percolation model with long-range correlations (Weinrib, 1984). Apart from the critical behavior that will depend on these correlations, one may wonder about the variation of the critical threshold. In a correlated percolation problem, the threshold is no longer a point but a line in a p vs. C_0 diagram. Because in our case both quantities are only functions of the same reduced variable $\xi_T[E]Dt$, one can be expressed as a function of the other. The very point at which the threshold line is crossed with increasing time, i.e., the point p_c reached at time t_{gel} at which the system percolates, is a constant independent of $\xi_T[E]Dt$. From Eq. 9, one obtains

$$t_{gel} \propto \frac{-ln(p_c)}{\xi_T D[E]}. \tag{11}$$

This expression shows how the gel degradation kinetics is intrinsically governed by the enzyme-diffusion process in the gel. In that sense, the gel degradation mechanism is diffusion- rather than reaction-limited. Note that this case is different from immobilized enzymes (Goldstein, 1976), for which an increasing distance enzyme-substrate is responsible for a diffusion-limited mechanism and anomalous kinetics.

For a simple diffusion due to Brownian motion, D being constant, we do not expect an anomalous dependence on enzyme concentration compared to a reaction-limited mechanism (Michaelis-Menten). However, in our case, the enzymes do not diffuse in a simple liquid but in a complex system which may strongly interact with them. A possible consequence of these interactions should be an anomalous subdiffusion process with a mean square displacement varying with time as $\langle r^2 \rangle \propto t^\beta$, with $\beta \leq 1$ ($\beta = 1$ corresponding to simple diffusion). The term ''subdiffusion'' refers to a decreasing apparent diffusion coefficient decreasing with time (or length scale) as $D(t) = d\langle r^2 \rangle / dt \propto t^{\beta - 1}$. Such behavior is quite usual in soft-matter physics and possible underlying mechanisms will be discussed in the following. Under the condition that the random walk pattern remains Gaussian but is anomalous only in its time dependence, our discussion concerning correlations remains valid. In particular, replacing the diffusion coefficient by $D(t)$ in Eq. 11 leads to

$$t_{gel} \propto [E]^{-1/\beta}, \tag{12}$$

which accounts for our result (see Fig. 1) for $\beta = 1/2$. In Fig. 6 we have reported the mean-square displacement of the enzyme in the gel that clearly show a subdiffusion behavior in the time window from 10^{-3} to 1 s with $\beta = 0.40$. Apart from the β-value that slightly differs, this is consistent with the results on gel degradation kinetics, provided this anomalous diffusion remains valid up to t_{gel}, i.e., up to $10^4 - 10^5$ s. This will be discussed in the following.

Anomalous enzyme diffusion

What is the possible origin of the subdiffusive dynamics of enzymes in the gel? As mentioned above, the mesh size of the gelatin network at this concentration is so large compared to the size of enzymes that they are not embedded in the gel network. This is confirmed by measurements on latex particles: despite a larger size they are free to move in the gel. In the absence of adsorption on gelatin, the enzymes are thus expected to freely diffuse in the gel. However, evidence for such adsorption is given by the enzyme stability that is enhanced in presence of gelatin (see Table 1). Such enzyme adsorption on the gel can be extrinsic and viewed as an usual protein-protein aggregation phenomenon, but it mainly comes from the intrinsic role of enzymes that form Michaelis complexes with the peptide bonds of the gel. Due to these interactions with the gel, the diffusion of the enzyme is necessarily slowed down and eventually anomalous. Let us give some estimates: 1% gelatin gel expressed in term of substrate concentration corresponds to $[S] \simeq 2 \times 10^{-2}$ M.

The Michaelis constant depends strongly on the local chemical structure involved in the neighboring of the recognition site. Typical values reported for thermolysin, but also on other proteases, lie between 10^{-4} and 10^{-3} M (Creighton, 1997; Pauthe, 1998). From Eq. 8, this results in a fraction of enzymes trapped in Michaelis complexes always being >95%. In other words, enzymes spend most of the time trapped onto the gel. Because the gel is immobile in a first approximation, an enzyme trapped on the gel is thus equally motionless. The time τ, needed for one gel network bond to be broken, is the sum of two contributions: the time τ_{dif} needed for one enzyme to freely diffuse in the solvent over ${\xi_T}^2$, and the time τ_{trap} spent when the enzyme is trapped on the gel into the volume ${\xi_T}^3$. From the above estimate one can neglect the former. The n steps' random walk of an enzyme can be viewed as a succession of n jumps from one trap to another (Bouchaud, 1992). At time t, the mean duration of one step is

$$\langle\tau\rangle = \int_0^t \tau_{trap} P(\tau_{trap}) d\tau_{trap}, \tag{13}$$

where $P(\tau_{trap})$ is the inherent distribution function of trapping times. This distribution comes naturally from the various combinations of $(Gly\text{-}X\text{-}Y)_n$ which can be encountered all along one gelatin filament and are so many potential Michaelis complexes with different lifetimes. The shape of this time distribution is directly related to the distribution of depths, ΔE, of potential wells associated to each trap. At least for the high values cutoff, it is reasonable to consider an exponential distribution of the energy barriers such as $P(\Delta E) = (1/E_0)e^{-\Delta E/E_0}$. Writing the trapping time as $\tau_{trap} = \tau_0 e^{\Delta E/kT}$, one gets

$$P(\tau_{trap}) \propto \tau_{trap}^{-(1+\beta)} \quad \text{with} \quad \beta = kT/E_0 < 1. \tag{14}$$

From Eq. 13, the resulting average τ-value is time-dependent, $\langle\tau\rangle = \propto t^{1-\beta}$. The enzyme diffusion process is a random walk of steps lasting $\langle\tau\rangle$, as

$$\langle r^2\rangle \propto t/\langle\tau\rangle \propto t^{\beta}. \tag{15}$$

This is consistent with our result in Fig. 6, but one may wonder about the time window within which such a behavior is expected, i.e., the width of the distribution $P(\tau_{trap})$.

For small peptide segments, depending on their length and chemical nature, values have been reported for $\tau_{cat} = {k_{cat}}^{-1}$ that vary from 10^{-3} up to 10^2 s and more (Pauthe, 1998). For nonspecific serine proteases, τ_{cat} values up to 10^4 s are reported (Creighton, 1997). When $K_m/[S] \ll 1$, i.e., when the majority of enzymes are trapped in Michaelis complexes, τ_{cat} gives a good estimate of an elementary trapping time τ_{trap}. Thus the corresponding width of the time distribution may usefully be compared to our FCS experiments. The above estimate for the τ_{trap} interval is fully compatible with the anomalous diffusion reported in Fig. 6 in a time interval between 10^{-3} and 1 s. In addition, this estimate supports the idea that the observed anomalous diffusion may extend at long time over several decades, and then fills the gap between FCS measurements and kinetics measurements. However, at very long time, i.e., beyond the longest trapping time, one actually expects to recover an usual diffusion behavior. A continuous crossover from an anomalous diffusion with $\beta = 0.4$ to this very long time behavior ($\beta = 1$) can explain the discrepancy between the β-values deduced from Figs. 6 and 1.

CONCLUSION

Experimental results on the kinetics of thermolysin-catalyzed degradation of gelatin gel have been reported as a function of enzyme concentration in the 1 nM range. The enzyme concentration dependence of the gel degradation time, t_{gel}, suggests both a diffusion-controlled mechanism and an anomalous subdiffusive motion of the enzymes in the gel. This last point was clearly underscored by two-photon fluorescence correlation spectroscopy measurements in the time window from 10^{-3} to 1 s. In view of the small size of enzymes compared to the mesh size of the network this anomalous diffusion is ascribed to adsorption of enzymes on gelatin chains rather than gel structure and heterogeneities as it was already observed by computer simulations (Netz and Dorfmüller, 1995). Actually, adsorption of enzymes on the gel is intrinsic to the catalytic action that necessarily involves their immobilization into Michaelis complexes. Further experiments are needed, and have been already initiated in our group, to get a direct evidence of the subdiffusive motion of enzymes up to the long timescale corresponding to gel degradation kinetics, i.e., up to t_{gel}, and to check whether this anomalous diffusion of the enzyme is closely related to its enzymatic activity.

From the theoretical point of view of the critical behavior of the reverse sol-gel transition, our results presumably imply a different universality class from percolation, which usually accounts for most of the gelation processes (Adam and Lairez, 1996). Actually, depending on correlations, different universality classes are theoretically expected (Weinrib, 1984), and numerically observed (Herrmann et al., 1982; Sahimi and Mukhopadhyay, 1996). Possible analogy with material fracture (Bouchaud, 1997) and/ or invasive percolation can also be suspected. Further experiments in this direction are needed.

The results here reported have to be taken into consideration in the framework of the ECM remodeling observed in metastasis dissemination. Tumor invasion implies the overexpression of proteinases (Murphy and Gavrilovic, 1999; McCawley and Matrisian, 2000) which degrade the ECM. The unusual anomalous diffusion-controlled mechanism of the gel degradation leads to a strong dependence of the apparent proteinase activity on enzyme concentration (the gel degradation velocity varies as

$[E]^2$). In other words, a small variation of proteinase concentration has a stronger effect than expected. In vivo, this would imply an amplification of the effects of proteinase overexpression.

APPENDIX: PERCOLATION GENERATED BY RANDOM WALKS

Consider a set of random walks between nearest neighbors on a three-dimensional lattice. The walks are initiated at points uniformly distributed with concentration $E = N_{walk}/N_{total}$ and are independent of each other. For each lattice site i, a variable $x_i(n)$ is defined as taking value *1*, if site i is visited by no walker after n steps for each of them, and value *0* otherwise. We have

$$\langle x_i(n)\rangle = \prod_\alpha \langle x_i^\alpha(n)\rangle = \langle x_i^\alpha(n)\rangle^{N_{walk}}$$

$$\langle x_i(n)x_j(n)\rangle = \prod_\alpha \langle x_i^\alpha(n)x_j^\alpha(n)\rangle = \langle x_i^\alpha(n)x_j^\alpha(n)\rangle^{N_{walk}},$$

where $x_i^\alpha(n)$ has the same definition for each walk α. Thus

$$\langle x_i(n)\rangle = exp\left[N_{walk} \times ln\left(1 - \frac{S(n)}{N_{tot}}\right)\right] \propto exp[-ES(n)]$$

and

$$\langle x_i(n)x_j(n)\rangle = exp\left[N_{walk} \times ln\left(1 - \frac{G_{ij}}{N_{tot}}\right)\right] \propto exp[-EG_{ij}(n)].$$

In these formulas $S(n) = 1 - \langle x_i^\alpha(n)\rangle$ is the mean number of sites visited by a walker after n steps and $G_{ij}(n)$ the probability that either i or j is visited after averaging over the initial point. The long time (large n) behaviors can be found from standard results on random walks (Barber and Ninham, 1970),

$$S(n) \propto (1 - R)n,$$

where R (*return probability*) is characteristic of the lattice, and G_{ij}, which is closely linked to the capture probability by traps located in i and j, is

$$G_{ij}(n) \propto 2S(n) + cst \times \frac{S(n)}{r_{ij}}.$$

We model the diffusion of enzymes in gelatin by random walks on a lattice standing for the gel network. The correspondence between real parameters and those of the above model is the cell parameter

$$\xi_T;\ E = [E]\xi_T^3;\quad n = Dt/\xi_T^2$$

(see Eqs. 9 and 10 in the text).

We thank G. Zalczer for numerous stimulating discussions; C. François for FCS prototype production; all the electronics staff; and particularly R. Daniel. The authors are also indebted to D. Furio and O. Benoist d'Azy for computer assistance. We sincerely thank the two reviewers for their valuable comments, which helped us to deepen this work and improve the manuscript.

REFERENCES

Adam, M., and D. Lairez. 1996. Physical Properties of Polymeric Gels: Sol-Gel Transition. John Wiley & Sons, Chichester, UK. 87–142.

Assoian, R. K. 1997. Anchorage-dependent cell cycle progression. *J. Cell Biol.* 136:1–4.

Barber, M., and B. Ninham. 1970. Random and Restricted Walks: Theory and Applications. Gordon and Breach, New York.

Basbaum, C. B., and Z. Werb. 1996. Focalized proteolysis: spatial and temporal regulation of extracellular matrix degradation at the cell surface. *Curr. Opin. Cell Biol.* 8:731–738.

Berry, H., and V. Larreta-Garde. 1999. Oscillatory behavior of a simple kinetic model for proteolysis during cell invasion. *Biophys. J.* 77:655–665.

Berry, H., J. Pelta, D. Lairez, and V. Larreta-Garde. 2000. Gel-sol transition can describe the proteolysis of extracellular matrix gels. *Biochem. Biophys. Arch.* 1524:110–117.

Bissell, M. J., and D. Radisky. 2001. Putting tumours in context. *Nat. Rev. Cancer.* 1:46–54.

Bouchaud, E. 1997. Scaling properties of cracks. *J Phys. Condens. Mat.* 9:4319–4344.

Bouchaud, J.-P. 1992. Weak ergodicity breaking and aging in disordered systems. *J. Phys. I France.* 2:1705–1713.

Browner, M., W. W. Smith, and A. L. Castelhano. 1995. Matrylisin inhibitor complexes: commons themes among metalloproteases. *Biochemistry.* 34:6602–6610.

Clerc, J.-P., G. Giraud, J. Roussenq, R. Blanc, J.-P. Carton, E. Guyon, H. Ottavi, and D. Stauffer. 1983. La Percolation. *Ann. Phys. Paris.* 8:4–105.

Creighton, T. E. 1997. Proteins. W. H. Freeman and Cie, New York.

Dallon, J. C., J. A. Sherratt, and P. K. Maini. 1999. Mathematical modelling of extracellular matrix dynamics using discrete cells: fiber orientation and tissue regeneration. *J. Theor. Biol.* 199:449–471.

DeClerck, Y. A. 2000. Interactions between tumor cells and stromal cells and proteolytic modification of the extracellular matrix by metalloproteinases in cancer. *Eur. J. Cancer.* 36:1258–1268.

Djabourov, M., N. Bonnet, H. Kaplan, N. Favard, J.-P. Lechaire, and M. Maillard. 1993. 3D analysis of gelatin gel networks from transmission electron microscopy imaging. *J. Phys. II France.* 3:611–624.

Eastoe, J. E., and A. A. Leach. 1977. The Science and Technology of Gelatin. Academic Press, London, UK.

Fadda, G. C., D. Lairez, and J. Pelta. 2001. Critical behavior of gelation probed by the dynamics of latex spheres. *Phys. Rev. E.* 63:61405.

Flory, P. 1953. Principles of Polymer Chemistry. Cornell University Press, Ithaca, NY.

Furie, B., and B. C. Furie. 1988. The molecular basis of blood coagulation. *Cell.* 53:505–507.

Gau, J. 2002. Dégradation enzymatique le gels de protéimes. Master's thesis. Université de Cergy-Pontoise.

Goldstein, L. 1976. Kinetic Behavior of Immobilized Enzyme Systems. Academic Press. 397–443.

Grams, F., P. Reinemer, J. C. Powers, R. Kleine, M. Pieper, H. Tschesche, R. Huber, and W. Bode. 1995. X-ray structures of human neutrophil collagenase complexed with peptide hydroxamate and peptide thiol inhibitors. *Eur. J. Biochem.* 228:830–841.

Guiot, E., M. Enescu, B. Arrio, G. Johannin, G. Roger, S. Tosti, F. Tfibel, F. Mirola, A. Brun, P. Georges, and M. P. Fontaine-Auparté. 2000. Molecular dynamics of biological probes by fluorescence correlation microscopy with two-photon excitation. *J. Fluoresc.* 10:413–420.

Herrmann, H. J., D. P. Landau, and D. Stauffer. 1982. New universality class for kinetic gelation. *Phys. Rev. Lett.* 49:412–415.

Hess, S., and W. Hebb. 2002. Focal volume optics and experimental artifacts in confocal fluorescence correlation spectroscopy. *Biophys. J.* 83:2300–2317.

Imanaka, T., M. Shibazaki, and M. Takagi. 1986. A new way of enhancing the thermostability of proteases. *Nature.* 324:695–696.

Krichevsky, O., and G. Bonnet. 2002. Fluorescence correlation spectroscopy: the technique and its applications. *Rep. Prog. Phys.* 65:251–297.

Larreta-Garde, V., and H. Berry. 2002. Modeling extracellular matrix degradation balance with proteinase/transglutaminase cycle. *J. Theor. Biol.* 251:105–124.

Matsubara, H. 1966. Observations on the specificity of thermolysin with peptides. *Biochem. Biophys. Res. Commun.* 24:427–430.

McCawley, L. J., and L. M. Matrisian. 2000. Matrix metalloproteinases: multifunctional contributors to tumor progression. *Mol. Med. Today.* 6:149–156.

Murphy, G., and J. Gavrilovic. 1999. Proteolysis and cell migration: creating a path? *Curr. Opin. Cell Biol.* 11:614–621.

Netz, P. A., and T. Dorfmüller. 1995. Computer simulation studies of anomalous diffusion in gels: structural and probe-size dependence. *J. Chem. Phys.* 103:9074–9082.

Pauthe, E. 1998. Approches Cinétiques et Moléculaires de la Reconnaissance Enzyme-Substrat: Application à l'Étude de l'Activité Protéolytique de la Thermolysine. PhD thesis. Université de Technologie de Compiègne, France.

Perumpanani, A. J., and H. M. Byrne. 1999. Extracellular matrix concentration exerts selection pressure on invasive cells. *Eur. J. Cancer.* 35:1274–1280.

Sahimi, M., and S. Mukhopadhyay. 1996. Scaling properties of a percolation model with long-range correlations. *Phys. Rev. E.* 54:3870–3880.

Weinrib, A. 1984. Long-range correlated percolation. *Phys. Rev. B.* 29:387–395.